Journal of Medicinal Chemistry

Article

Discovery of (3-(4-(2-oxa-6-azaspiro[3.3]heptan-6-ylmethyl)phenoxy)azetidin-1-yl)(5-(4-methoxyphenyl)-1,3,4-oxadiazol-2-yl)methanone (AZD1979), a melanin concentrating hormone receptor 1 (MCHr1) antagonist with favourable physicochemical properties

Anders Johansson, Christian Löfberg, Madeleine Antonsson, Sverker von Unge, Martin Hayes, Robert Judkins, Karolina Ploj, Lambertus Benthem, Daniel Lindén, Peter Brodin, Marie Wennerberg, Marléne Fredenwall, Lanna Li, Joachim Persson, Rolf Bergman, Anna Pettersen, Peter Gennemark, and Anders Hogner

J. Med. Chem., **Just Accepted Manuscript** • DOI: 10.1021/acs.jmedchem.5b01654 • Publication Date (Web): 07 Jan 2016

Just Accepted

ACS Publications

Journal of Medicinal Chemistry is published by the American Chemical Society. 1155 Sixteenth Street N.W., Washington, DC 20036

Discovery of (3-(4-(2-oxa-6-azaspiro[3.3]heptan-6-ylmethyl)phenoxy)azetidin-1-yl)(5-(4-methoxyphenyl)-1,3,4-oxadiazol-2-yl)methanone (AZD1979), a melanin concentrating hormone receptor 1 (MCHr1) antagonist with favourable physicochemical properties

Anders Johansson, Christian Löfberg, Madeleine Antonsson, Sverker von Unge, Martin A. Hayes, Robert Judkins, Karolina Ploj, Lambertus Benthem, Daniel Lindén, Peter Brodin, Marie Wennerberg, Marléne Fredenwall, Lanna Li, Joachim Persson, Rolf Bergman, Anna Pettersen[#], Peter Gennemark and Anders Hogner*

Cardiovascular & Metabolic Diseases iMed and [#]Global Medicines Development, AstraZeneca Gothenburg, 431 83 Mölndal, Sweden.

ABSTRACT: A novel series of melanin concentrating hormone receptor 1 (MCHr1) antagonists were the starting point for a drug discovery program that culminated in the discovery of **103** (AZD1979). The lead optimisation program was conducted with a focus on reducing

lipophilicity and understanding the physicochemical properties governing CNS exposure and undesired off-target pharmacology, such as hERG interactions. An integrated approach was taken where the key assay was *ex vivo* receptor occupancy in mice. The candidate compound **103** displayed appropriate lipophilicity for a CNS indication and showed excellent permeability with no efflux. Preclinical GLP toxicology and safety pharmacology studies were without major findings and **103** was taken into clinical trials.

Introduction

Obesity is one of the underlying causes of several serious conditions such as type II diabetes, coronary heart disease, high blood pressure, liver disease and cancer.[1] Over the last 15 years, great efforts have been devoted to finding effective, safe and easy to use weight loss medications[2] and much of the attention has been directed towards appetite control.[3] The cyclic 19 amino acid neuropeptide MCH is associated with feeding behavior.[4] It activates the MCH receptor1 (MCHr1) located in the hypothalamus. The receptor is also known as the human orphan G-protein coupled receptor SLC-1 or GPR24.[5] Mice lacking MCH are lean and hypophagic.[6] It has been shown independently by several groups that MCHr1 knockout (KO) mice are resistant to dietary induced obesity (DIO) mainly due to elevated motor activity and energy expenditure.[7] Small molecule MCHr1 antagonists have been discovered and the effect observed on body weight is in accordance with those for KO animals.[8] However, while experimental data in rodents are supportive, human translation remains unconfirmed.[9] In non-rodents, the picture is complicated by expression of a second MCH receptor, MCHr2,[10] for which a role has yet to be defined.[11] Only very limited data is available in the literature on food intake/weight loss in MCHr2 expressing species[12] and only recently a selective MCHr2

antagonist was disclosed.[13] Although the main attention of MCHr1 antagonists has been drawn to their potential for the treatment of obesity, other biological effects are also worth mentioning. For instance, MCHr1 antagonists have been investigated preclinically as a treatment option for depression and anxiety disorders.[14] Furthermore, an MCHr1 antagonist has been shown to alleviate steatohepatitis[15] and MCHr1 KO mice are resistant to seizures.[16]

The established connection between the MCHr1 system and weight control in rodents has stimulated extensive efforts in the drug discovery of small molecules as MCH receptor antagonists.[17] Despite being an attractive target for indications such as obesity and depression/anxiety, a major hurdle has been to identify a chemical series with attractive physicochemical properties. A large number of published MCHr1 antagonists are lipophilic bases. Not surprisingly, one known liability for many programs has been to circumvent interactions with the hERG channel.[18] However, not only is it necessary to achieve a large enough separation between MCHr1 and hERG, but this also needs to be accomplished without impairing necessary CNS exposure.[19] This presents quite a challenge.[20]

Results and discussion

Following an earlier MCHr1 program at AstraZeneca,[21] a new high throughput screen (HTS) looking for compounds binding to MCHr1 was run on a subset of the AstraZeneca compound collection. The HTS was run looking for functional antagonists using a high throughput FLIPR assay.[22] Special attention was paid to include all compounds added to the collection since the previous HTS in the earlier program. Amongst the hits, one series was identified which was considered to possess promising physicochemical properties. To guide continued chemistry efforts a functional primary assay was preferred and a [^{35}S]GTPγS assay was developed for

MCHr1 and used throughout the program.[23] The lead identification chemistry culminated in compound **1**, which was the starting point for the lead optimisation program. A summary of the key properties of **1** is given in **Table 1**. An analysis of the physicochemical property space of known MCHr1 antagonists was made. Physicochemical properties were calculated for all publicly disclosed MCHr1 antagonists, including compounds from patent applications derived from the online database GOSTAR.[24] This gave an average clogP of 5.2 and an average polar surface area (PSA) of 54.[25] The physicochemical properties of **1** contrasted to the physicochemical property space of published MCHr antagonists and suggested it to be a good starting point. Additionally, and even more importantly, this compound and the series it represented had high passive permeability as assessed in Caco2 cells and exhibited no

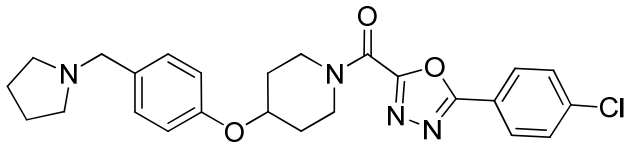

1

Table 1. *In vitro* data for compound 1

IC_{50} MCH GTPγS (nM)[a]	IC_{50} MCH bind. (nM)	IC_{50} hERG (μM)	Solubility[b] (μM)	logD[c] (ClogP)	PSA[d]	pKa (calc)	LLE[e]	Caco AB[f] (Efflux ratio)	IC_{50} CYP min (3A4)	HLM Clint[g]	RLM Clint[g]
20	11	5.5	70	3.4 (2.9)	63	9.8	4.3	43 (0.37)	5.2	13	17

[a] Functional potency.[23] [b] Solubility at pH 7.4 from DMSO solution. [c] $LogD_{7.4}$ hplc [d] Polar Surface Area [e] LLE calculated from pIC50 MCH GTPγS minus logD. [f] 10^{-6} cm/s [g] μl/min/mg

efflux. This suggested a lack of interaction with efflux transporter proteins and the potential to achieve high exposure in the CNS. A deeper understanding of target engagement in the CNS can be attained by measuring receptor occupancy in the regions of interest in the brain. Although the receptor expression level of MCHr1 is quite low both in both rodents and humans,[26] ligands that are useful for measuring *ex vivo* receptor occupancy (RO) have been reported.[27] Our RO model was based on the use of [^{3}H](S)-methyl 3-(3-(4-(3-acetamidophenyl)piperidin-1-yl)propylcarbamoyl)-4-(3,4-difluorophenyl)-6-(methoxymethyl)-2-oxo-1,2,3,4-tetrahydropyrimidine-5-carboxylate ([^{3}H]-SNAP-7941) as radioligand.[28] After *po* administration of 50 μmol/kg of **1** to mice a MCHr1 receptor occupancy of more than 90% could be detected, thus providing evidence of compound exposure and target coverage in the CNS. The lead compound and the series it represents contained an amide bond, which was not completely stable to amidase hydrolysis when measuring rat and mouse plasma protein binding data using a standard method. However, by shortening the equilibration time in the assay this could be overcome. Hydrolytic cleavage was never observed when analysing plasma samples from *in vivo* studies. Further *in vivo* assessment of the compound included a 21 day weight loss study in diet induced obese (DIO) mice, where a dose related decrease in body weight was observed. However, the compound contained the three-point hERG pharmacophore[29] with two aromatic rings and a basic nitrogen and showed an IC_{50} of 5 μM on the hERG channel. Although no acute CV findings were detected *in vivo* in anaesthetized guinea pigs, a reduction in hERG was considered an improvement parameter for the lead optimisation program. A move to non-basic compounds can be a strategy for removing hERG interactions.[30] However, in this series, without exception, replacing the basic N with amide functionalities resulted in loss or severe decline in MCHr1 potency. This change also moved compounds into more lipophilic physicochemical

space, where the most lipophilic variants in some cases displayed hERG activity in the low micro molar range, despite the absence of a basic N. The physicochemical properties of **1** are a good starting point, with a logD of 3.4, a solubility of 70 µM and an attractive permeability profile. Whilst the basic N appeared to be an integral part of the lead, we hypothesized that it should be possible to modify chemistry in the series to achieve a wide enough margin over the hERG channel by driving down lipophilicity to minimize hERG interactions and other potential off target pharmacology.

Chemistry

The lead series was divided into three distinct regions as shown in **Figure 1**. SAR investigations took advantage of the synthetic flexibility in terms of selection of last step coupling to provide the final compound. Final compounds were prepared either by an amide formation between the

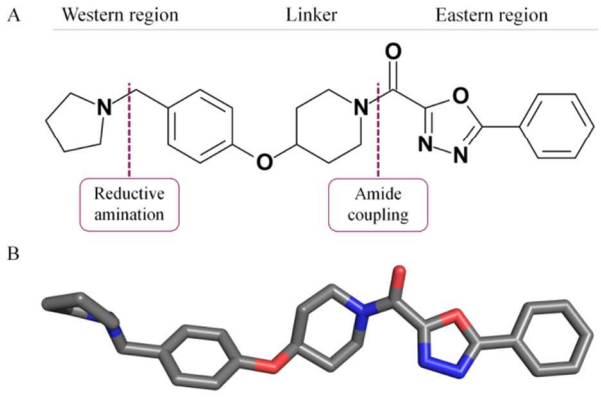

Figure 1. (A) Series regions and coupling strategies for MCH1r lead series. **(B)** Low energy conformation of **1** used as 3D-hypothesis for SAR analysis.

secondary N of the linker region and an eastern region ester/acid or the final step was a reductive amination of a benzylic aldehyde, by which the western region amine was introduced last. A

third option was to form the ether bond as the last step by a nucleophilic displacement reaction. This was less frequently used in the lead optimization program, but could be applied with good atom economy when preparing larger batches for toxicological studies.

Preparation of final compounds using amide formation as the last step started with preparation of western amine fragments as shown in **Scheme 1**. Reductive amination of a 4-hydroxybenzaldehyde with the selected amine using $Na(CH_3CO_2)_3BH$ and triethylamine in

Scheme 1[a] Synthesis of building blocks **4, 6, 9, 12, 15, 18, 21, 25, 28, 31, 34, 37.**

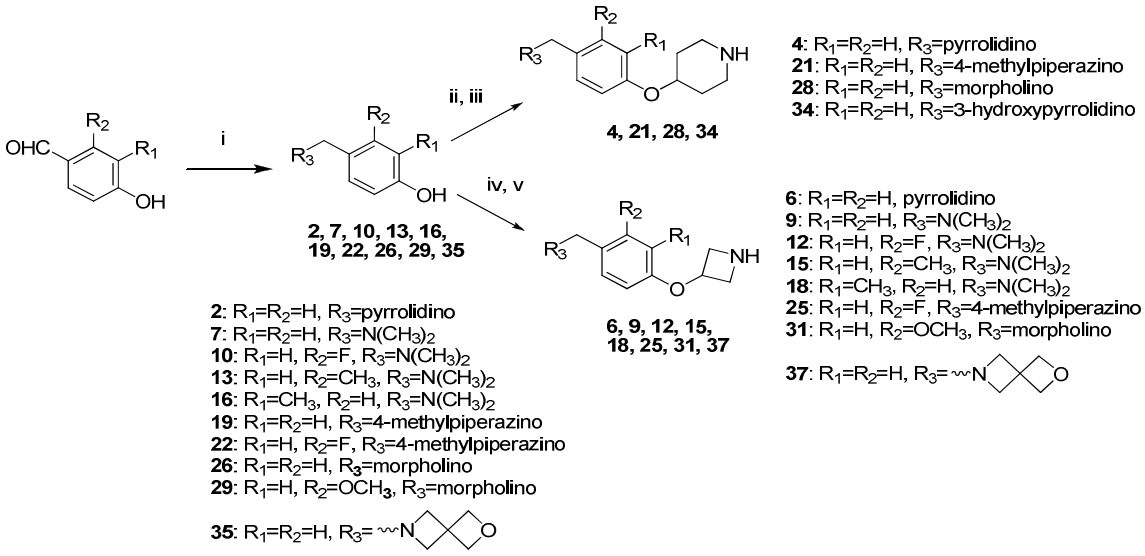

[a]Reagents and conditions: (i) Amino compound, $Na(CH_3CO_2)BH$, TEA, DCM, rt (81-96%); (ii) Ph_3P, *tert*-butyl 4-hydroxypiperidine-1-carboxylate, DIAD, DCM, 0°C → rt (77-93%); (iii) The N-Boc deprotection was accomplished by different techniques for different compounds. Synthetic details are presented in the Experimental section; (iv) NaH or Cs_2CO_3, *tert*-butyl 3-[(methylsulfonyl)oxy]-azetidine-1-carboxylate, DMF, 80-90°C (55-99%). Compound **22** was synthesized using 2-fluoro-4-methoxybenzaldehyde during a reductive amination step followed

by an ether hydrolysis.; (v) The *N*-Boc deprotection was accomplished by different techniques for different compounds. Synthetic details are presented in the Experimental section. Compound **34** was synthesized in a reversed fashion, i.e. (i) Mitsunobu reaction (52%); (ii) Reductive amination (76%); (iii) *N*-Boc deprotection (67%).

dichloromethane provided the *p*-hydroxy benzylamine products in good yield. Substitutions in the phenyl region were generally well tolerated and the method could be used for a variety of amines, from dimethyl amine and pyrrolidine to the less nucleophilic morpholine and piperazine. The western amine fragment was then connected *via* formation of an ether to a piperidine or azetidine linker. Two different methods were utilized to accomplish this ether formation. Piperidine building blocks were prepared using a Mitsunobu reaction between the *p*-hydroxy benzylamine and 4-hydroxy Boc-piperidine followed by Boc-deprotection. Azetidine ethers were prepared by O-alkylation of the *p*-hydroxy benzylamine by Boc-protected azetidin-3-mesylate, in the presence of NaH or Cs_2CO_3, followed by acidic hydrolysis of the Boc-group. The reaction order could also be reversed, as exemplified by **34**, where the Mitsunobu reaction between Boc-piperidin-4-ol and 4-hydroxybenzaldehyde was performed first, followed by reductive amination

Scheme 2[a] Conditions for amide formation.

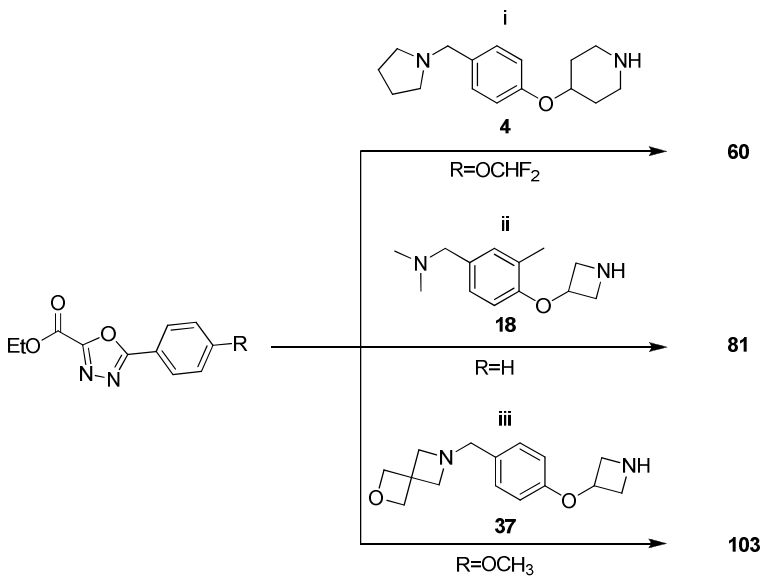

[a]Reagents and conditions: (i) R=$OCHF_2$, 4-(4-(Pyrrolidin-1-ylmethyl)phenoxy)-piperidine (**4**), EtOH, reflux 20h, 37%. (ii) R=H, 1-(4-(Azetidin-3-yloxy)-3-methylphenyl)-N,N-dimethylmethanamine (**18**), neat, 120 °C, 3h, 57%. (iii) R=MeO, 6-(4-(azetidin-3-yloxy)benzyl)-2-oxa-6-azaspiro[3.3]heptane (**37**), catalytic NaCN, MeOH, rt, 2h, 65%. The structures of **60**, **81** and **103** are shown in **Table 2**, **Table 4** and **Table 6**, respectively

and deprotection. Amide formation could be accomplished in several ways. However, since the 1,3,4-oxadiazole carboxylic acids decarboxylate spontaneously at room temperature, standard coupling reagents could not be used and therefore coupling reactions were performed with ethyl esters. The different conditions used are summarized in **Scheme 2.** The reaction conditions utilized initially (**Scheme 2**, i) worked well for R= *p*-Cl or other electron withdrawing substituents. However, for electron rich 1,3,4-oxadiazole esters, where R= *p*-MeO, these conditions suffered from long reaction times along with significant by-product formation. For example, considerable amounts of 2-phenyl-1,3,4-oxadiazole was formed by hydrolysis of the ester, followed by decarboxylation. To avoid these problems an alternative protocol was developed (**Scheme 2**, ii). In this protocol, the amine building block was allowed to react with

the 1,3,4-oxadiazole ester under solvent-free conditions (neat) at 120 °C for 2-3h. This procedure provided rapid and straightforward access to final compounds with a cleaner reaction profile, improved reaction times and easier purification. Often, the final compounds were crystallized directly from the crude reaction mixture. Reaction conditions were not optimized for each individual compound. However, a further improved method was developed (**Scheme 2**, iii). The mild NaCN catalysed coupling of the amine to the 1,3,4-oxadiazole phenyl ester at room temperature.[31] This method became the preferred method as the program developed. Many other heterocycles in the eastern region were stable as carboxylic acids and therefore classic amide coupling conditions were employed (**Scheme 3**). It is worth noting that the 1,2,4-oxadiazole phenyl amides also were prepared by coupling to corresponding methyl esters.

Scheme 3[a] Synthesis of analogues **63-67**.

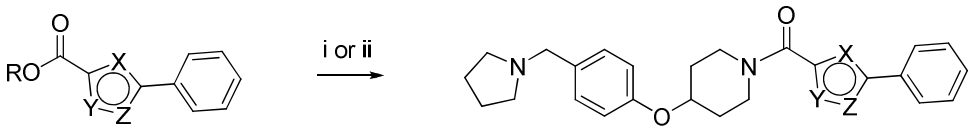

R=H, Me, Et **63-67**

[a]Reagents and conditions: (i) For compounds **63, 65** and **66: 4**, EDC, DMAP, DCM, rt (65-72%); (ii) For compounds **64** and **67: 4**, NaCN (cat), MeOH, rt (52-83%). For detailed structural information of compound **63-67**, see **Table 3**.

For synthesis of piperidine linked western pyridines, the synthetic routes were modified. Preparation of **46** started with reductive amination of 6-chloronicotinaldehyde with pyrrolidine using $Na(CH_3CO_2)_3BH$ and triethylamine in dichloromethane (**Scheme 4**). Nucleophilic

displacement of Cl with Boc-protected 4-hydroxypiperidine in the presence of NaH in DMSO

Scheme 4[a] Synthesis of pyridine analogue **46**.

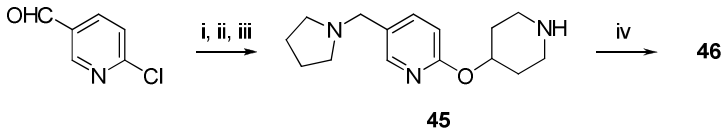

[a]Reagents and conditions: (i) Pyrrolidine, $Na(CH_3CO_2)_3BH$, TEA, DCM, rt (79%); (ii) *tert*-butyl 4-hydroxypiperidine-1-carboxylate, NaH, DMSO, 70°C (57%); (iii) TFA, DCM, rt (92%); (iv) Ethyl 5-(4-methoxyphenyl)-1,3,4-oxadiazole-2-carboxylate, EtOH, reflux (48%). Compound **46** is shown in **Table 4**.

and subsequent deprotection using TFA in dichloromethane gave intermediate **45.** Amide formation with the *p*-methoxyphenyl oxadiazole ester in refluxing ethanol afforded **46**.

Synthesis of the pyridine analogue **51** started with formation of the acid chloride of 5-hydroxypicolinic acid, using thionyl chloride. Treatment with pyrrolidine gave the corresponding amide (**Scheme 5**). Subsequent reduction of the amide to amine was accomplished using $(CH_3)_2S{\cdot}BH_3$ in THF. Mitsunobu coupling followed by deprotection of the Boc-group gave **50**, which was finally converted to **51** by treatment with *p*-methoxyphenyl oxadiazole ester under solvent-free conditions at 120 °C.

Scheme 5[a] Synthesis of pyridine analogue **51**.

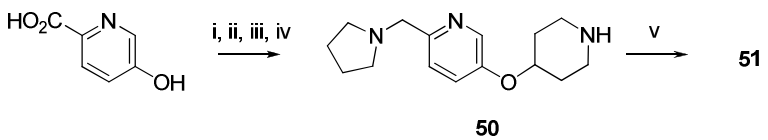

[a]Reagents and conditions: (i) $SOCl_2$, DCM, reflux 3 h, then pyrrolidine, rt (25%); (ii) $(CH_3)_2S{\cdot}BH_3$, THF, 0°C → rt, then MeOH; (iii) Ph_3P, *tert*-butyl 4-hydroxypiperidine-1-carboxylate, DIAD, THF, 0°C → rt (35%, two steps); (iv) TFA, DCM, rt (46%); (v) Ethyl 5-(4-methoxyphenyl)-1,3,4-oxadiazole-2-carboxylate, neat, 120°C (38%). Compound **51** is shown in **Table 4**.

The linear synthetic sequence culminating in a reductive amination reaction to form the final compounds was employed most widely throughout the program, as the largest number of variations was investigated in the western part of the molecule and this route introduces diversity in this part of the molecule as the last step (**Scheme 6)**. The common aldehyde building blocks were prepared starting from the desired phenylic 1,3,4-oxadiazole ester, which was treated with 3-hydroxyazetidine, catalytic amounts of NaCN and triethylamine in methanol to form the corresponding 3-hydroxyazetidine amides in good yield. The free hydroxyl group was readily converted to a mesylate, under standard conditions, to afford **53** and **56** in high yield.

Scheme 6[a] Synthesis of building blocks **54, 57.**

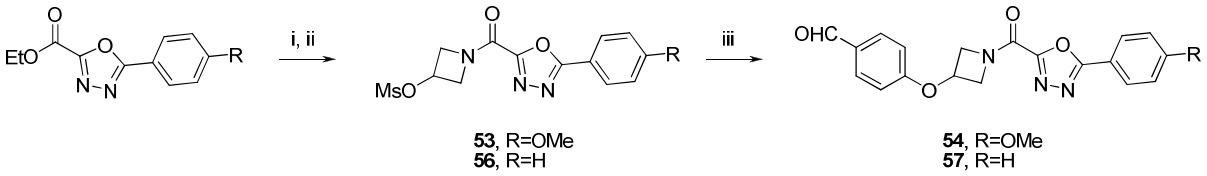

53, R=OMe
56, R=H

54, R=OMe
57, R=H

[a]Reagents and conditions: (i) NaCN, 3-hydroxyazetidinium chloride, TEA, MeOH, rt (77-87%); (ii) TEA, MsCl, DCM, 0°C → rt (77-99%); (iii) 4-hydroxybenzaldehyde, Cs_2CO_3, DMA, 110°C (54-75%).

Finally, the aldehyde intermediates **54** and **57** were obtained by O-alkylation of 4-hydroxybenzaldehyde with **53** and **56** in the presence of Cs_2CO_3 in DMA at 110 °C. These

western aldehyde building blocks were then converted into a variety of target benzylic amines *via* a reductive amination step as shown in **Scheme 7**.

Scheme 7[a] Synthesis of analogues **89**, **90**, **94**, **97**, **98**, **99**, **100**, **101**, **102**, **103** by a reductive amination as the final step.

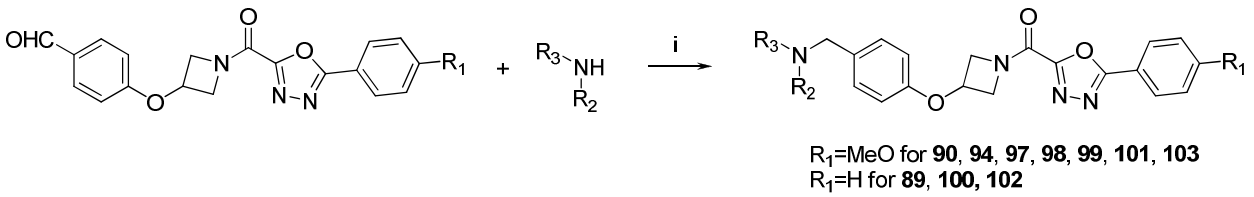

[a]Reagents and conditions: (i) $Na(CH_3CO_2)_3BH$, TEA, DCM, 0 °C → rt (17-76%). The structures of the target benzylic amines are shown in **Tables 5** and **6**.

Structure activity relationships and discovery of the clinical candidate 103 (AZD1979)

The reported MCHr1 pharmacophore with a planar elongated structure containing a hydrophobic aromatic moiety, a hydrogen bond acceptor, and a positively charged site appeared to be relevant for the chemical series.[18, 32] However, a more detailed hypothesis of a putative bioactive conformation of **1** arose from a conformational analysis of a set of published MCH1r antagonist structures.[33] Low-energy conformations of each molecule were generated, and subsequently pair-wise shape-based alignments were performed.[34] This resulted in a number of molecular alignments, where visual inspection favored the alignment shown in **Figure 1b**, since it allowed the rationalization of series specific SAR within the chemical series. This molecular alignment served as an initial working 3D-hypothesis for SAR analysis and the 3D model was in line with the characteristics of the reported MCHr1 pharmacophore.

Table 2. Eastern phenyl substitutions

Compound	Structure	IC_{50} MCH GTPγS[a] (nM)	IC_{50} hERG (μM)	Solubility[b] (μM)	logD[c] (ClogP)	Caco AB[d] (Efflux ratio)	HLM Clint[e]	LLE[f]
58	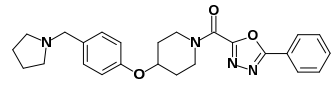	43	11.0	>100	2.2 (2.2)	55 (0.28)	S	5.2
59	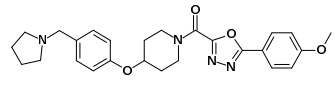	28	11.0	>100	2.3 (2.2)	46 (0.23)	S	5.3
60	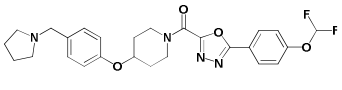	15	4.2	ND	2.9 (2.7)	50 (0.21)	15	4.9
61	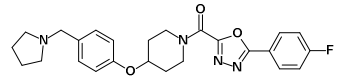	44	6.2	>100	2.4 (2.3)	52 (0.3)	S	5.0
62	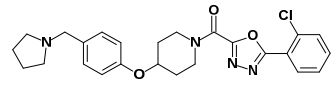	1000	5.3	ND	2.7 (2.7)	59 (0.34)	13	3.3

[a] Functional potency.[23] [b] Solubility at pH 7.4 from DMSO solution. [c] $LogD_{7.4}$ hplc [d] 10^{-6} cm/s [e] μl/min/mg [f] LLE calculated from pIC50 MCH GTPγS minus logD. ND Not determined S Stable to assay conditions (100% parent compound remaining after incubation)

Initially, attention was turned to the eastern region of the molecules. An early assessment of the series included replacements for the *p*-Cl substituent, which gratifyingly proved not to be essential for MCHr1 potency. As shown in **Table 2**, MCHr1 potency does not vary significantly between *para*-substituted phenyls in the eastern region. However, a marked drop in potency could be observed for other substitution patterns. In line with the 3D working hypothesis, *o*-Cl-phenyl **6** forces the phenyl group out of plane. This drastically affects the MCHr1 potency and indicates that the MCHr1 site is complementary to the planar shape of the distal phenyl ring.

Permeability and efflux characteristics, as measured in Caco2 cells, did not differ with modifications in the eastern phenyl region, as all variants showed high Caco2 permeability with no signs of efflux. Furthermore, metabolic stability *in vitro* in both rat and human liver microsomes was improved when the Cl-substituent was replaced. For example, phenyl derivative **58** and *p*-MeO-phenyl derivative **59** were both completely stable in both rat and human liver microsomal incubations. Additionally, **59** did not show any sign of CYP450 inhibition against any of the CYP450's measured (CYP1A2, CYP3A4, CYP2C8, CYP2C9, CYP2C19, and CYP2D6). Within this set of compounds, *p*-phenyl substitution showed small variations in hERG potency. However, when taking measured logD into account and calculating lipophilic ligand efficiency (LLE), the unsubstituted phenyl derivative **5** and *p*-MeO-phenyl derivative **6** were considered most promising. Both **58** and **59** gave a small decrease in hERG potency and, in combination with the highest LLE values, made these variations attractive for further exploration. Hence, it was reasoned that these would provide the lowest baseline lipophilicity and unsubstituted phenyl and *p*-MeO-phenyl were chosen as eastern substituents for SAR expansion of the other regions of the molecule.

Table 3. Eastern region heterocycles

Compound	Structure	IC_{50} MCH GTPγS[a] (nM)	IC_{50} hERG (μM)	Solubility[b] (μM)	logD[c] (ClogP)	HLM Clint[d]	LLE[e]
63	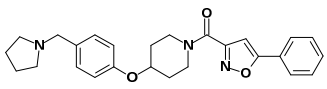	61	3.3	198	3.0 (3.6)	S	4.2
64	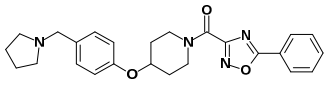	150	7.5	991	2.6 (2.8)	6	4.2

65	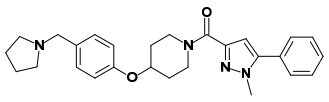	I	7.4	930	2.2 (3.5)	7	NA
66	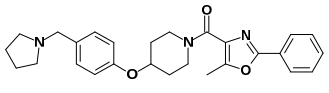	1200	3.0	754	3.0 (3.5)	S	2.9
67	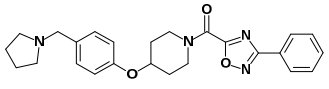	75	1.8	<0.005	3.2 (2.8)	S	3.9

[a] Functional potency.[23] [b] Solubility at pH 7.4 from DMSO solution. [c] $LogD_{7.4}$ hplc [d] µl/min/mg [e] LLE calculated from pIC50 MCH GTPγS minus logD. S Stable to assay conditions (100% parent compound remaining after incubation) I Inactive

In the heterocyclic eastern region, several five membered ring heterocycles were investigated (**Table 3**). However, the 1,3,4-oxadiazole **58** proved to best combine physicochemical properties and MCHr1 potency. Displaying the lowest lipophilicity of the heterocycles investigated, the 1,3,4-oxadiazole **58** also gave the greatest separation between MCH potency and hERG activity. In addition, the LLE was the highest of the heterocycles examined. There is a remarkable variation in solubility and measured logD between the 1,3,4-oxadiazole and one of the two isomeric 1,2,4-oxadiazoles, **67**.[35] The difference in activity on the hERG channel between **58** and **67** is also noteworthy. Changing the shape and electrostatic properties by substitution on the 5-membered heterocyclic rings in **65** and **66** were not beneficial for MCHr1 potency, again emphasizing the importance of the planar shape complementarity towards this part of the MCHr1 cavity.

Whilst the chemical series showed great potential for further optimization, an effective screening cascade was required to direct the chemistry efforts. In the first wave of the screening cascade,

MCHr1 potency was assessed using a functional GTPγS assay. The first wave of basic data also included parallel generation of data on physicochemical properties, hERG activity and fundamental DMPK properties, e.g. metabolic stability and CYP450 inhibition. As *in vitro* Caco2 permeability data did not provide sufficient guidance to funnel compounds through the screening cascade, the *ex vivo* receptor occupancy assay in mice was introduced as a routine screening model.[27c] Compounds that progressed into the receptor occupancy (RO) assay were also investigated in a binding assay on mouse MCHr1 for correlation with the free RO IC_{50} values. Although *in vitro* permeability data did not differ substantially within the chemical series, large variations in the degree of RO were observed. Free concentrations of compound in brain or cerebrospinal fluid were not measured on a routine basis, but instead RO values were related to unbound plasma concentrations to drive the chemistry effort. Mice were administered *po* a fixed dose of compound and euthanized after different time points ranging from 15 minutes to 24 hours after dosing. The RO experimental model was used with a 10 day cycle time and the data (*ex vivo* RO vs. unbound plasma concentration) were analyzed by fitting a simple E_{max} model to the data, resulting in an estimate of apparent *in vivo* IC_{50}. The RO data served two purposes. It provided an understanding of the difference in the level of target engagement between different compounds and guided dose setting in the longer *in vivo* disease model experiments, such as weight loss measurements in chronic (3 weeks) treatment in diet-induced obese (DIO) mice. The receptor occupancy assay can be described as the gate keeper assay in the program, offering both ranking between compounds and dose setting for longer *in vivo* studies, as well as providing guidance for the design of molecules with improved properties.

The focus to move chemistry to a lower lipophilicity range prompted the investigation of azetidines in the linker region. According to the 3D working hypothesis, the azetidines would

still adopt a planar distal eastern region and also position the basic N in a similar position to compound **1**. Indeed, the piperidine linker could be contracted to an azetidine, which combined a general improvement in MCHr1 potency with lower lipophilicity. However, despite the shift towards lower lipophilicity with the azetidine linker, there was not a general shift towards decreased interactions with the hERG channel. Whilst there was no actual gain in the MCHr1 to hERG ratio between matched piperidine-azetidine pairs, the focus of the chemistry efforts now turned to the western region of the molecule and the lower baseline lipophilicity provided by moving to an azetidine linker gave a greater degree of freedom for exploring the western region. In addition, there was a better correlation between measured *in vitro* binding data and RO for the azetidine linked compounds. Although the piperidine linkers have been revisited by matched pair synthesis throughout the program, the focus of the chemistry effort was shifted towards the azetidine linker. Pyrolidine linkers were also investigated as an alternative, but did not offer any improvement over piperidine or azetidine linkers. In fact, both CYP inhibition and hERG potency went in the wrong direction for both enantiomers of the pyrolidine rings. Functional potency as measured in the MCHr1 GTPγs assay was in the same range as for the azetidines and piperidines.

As suggested by the 3D working hypothesis, the western region of the molecules proved to be the most tolerant to structural modifications and, hence, became the region to which the majority of chemistry modification was dedicated. Initially, we were interested in reducing the size of the western region and it was possible to replace the pyrrolidine ring with dimethyl amines, without eroding MCHr1 potency (compound **77**, **Table 4**). In a sense, this can be regarded as the minimized lead structure. However, this did not result in an increased margin over hERG and

Table 4. Western modifications

Compound	Structure	IC_{50} MCH $GTP\gamma S$[a] (nM)	IC_{50} MCH bind Mu (nM)	IC_{50} RO, free[b] (nM)	IC_{50} hERG (μM)	logD[c]	pKa[d]	Caco AB[e] (Efflux ratio)	HLM Clint[f]	RLM Clint[f]
76	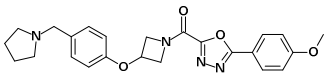	34	6	4	5.5	1.8	9.9	35 (0.37)	21	40
77	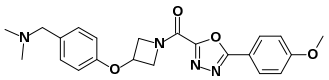	29	13	14	21	1.55	8.9[g]	67 (0.29)	17	53
78	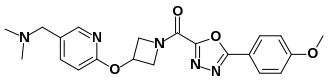	200	ND	ND	>33	1.8	8.5	ND	13	145
46	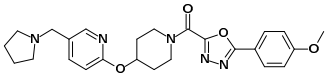	140	ND	ND	>33	2.3	9.2	49 (0.25)	24	28
51	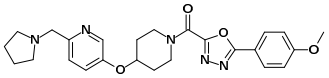	220	ND	ND	25	1.8	9.1	31 (0.39)	S	S
79	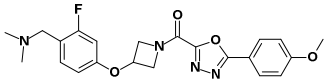	22	15	9	15	2.2	8.6	62 (0.32)	42	218
80	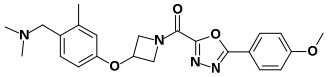	23	14	1	10	2	9.3	54 (0.30)	22	149
81	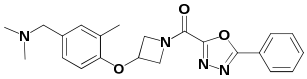	21	9	5[h]	8.6	1.9	9.3	62 (0.32)	S	54

[a] Functional potency.[23] [b] RO receptor occupancy. IC_{50} relates to free plasma levels. [c] $LogD_{7.4}$ hplc [d] Experimental pKa[36] [e] 10^{-6} cm/s [f] μl/min/mg [g] calculated value [h] Human plasma protein binding used to calculate IC_{50} RO, free. ND Not determined S Stable to assay conditions (100% parent compound remaining after incubation)

demethylation of the western amines became an additional metabolic route, primarily in rodents, which made the evaluation of these compounds complex. Substitutions in the western phenyl region were investigated for two reasons: to tune pKa and to investigate restrictions of this flexible part of the molecule. We speculated that both of these effects individually or combined could be a way to increase the margin between MCHr1 and hERG activity. A decrease in pKa would reduce the affinity towards the hERG channel and conformational restrictions could potentially increase the population of MCHr1 preferred conformations. Introduction of a pyridine ring in the aromatic western region reduced pKa of the western amines, most notably in **78**. The lower pKa also led to a reduced hERG activity, but also resulted in lower MCHr1 potency. With other changes in the western phenyl region, there was no clear correlation between hERG potency and pKa, but a majority of compounds with a reduced pKa showed a lower hERG activity. RO IC_{50} correlated well with measured *in vitro* binding IC_{50} in mice, indicating a lack of CNS efflux. However, it is noteworthy that methylation of the western phenyl region in some cases showed a marked increase in potency in the RO model, as compared to the *in vitro* binding value. This effect was consistently observed in methylated western phenyls such as in **80**. The increase in potency could be translated to *in vivo* experiments and RO IC_{50} was used to set the dose for these studies. The main hurdle with these structural modifications proved to be combining metabolic stability with an increased margin to hERG activity. For example, removing the methoxy substituent in the eastern region as in compound **81** resulted in an increased metabolic stability, but this modification made the compounds more active on the hERG channel.

Cyclic amine substituents with lower pKa were then investigated (**Table 5**). Introduction of piperazine rings showed lower levels of hERG interaction (e.g. as in compounds **83** and **84**), but

did not give the required MCHr1 potency. Although not consistent for all western piperazines, metabolic stability worsened in some cases with these modifications. This effect was more pronounced for morpholine substituents, as shown with compounds **85** and **86**. The logD increase observed with the lower pKa morpholines completely eroded metabolic stability. Introduction of a hydrogen bond donor (HBD) in the western region in the form of hydroxy substituted pyrolidines resulted in compounds with good MCHr1 potency, a lower level of hERG interaction and acceptable metabolic stability (**Table 5**, compounds **87, 88, 89, 90** and **91).** However, despite Caco2 efflux values indicating a low degree of efflux, the introduction of an HBD had a detrimental effect on RO. Attempts were made to mask the hydroxyl substituent by geminal or vicinal methylation, but this was unsuccessful.

Even if cut-off values for physicochemical properties such as logD or pKa, could not be firmly

Table 5. Western modifications: pKa modifications

Compound	Structure	IC_{50} MCH $GTP\gamma S$[a] (nM)	IC_{50} MCH bind Mu (nM)	IC_{50} RO, free[b] (nM)	IC_{50} hERG (μM)	logD[c] (ClogP)	pKa[d]	Caco AB[e] (Efflux ratio)	HLM Clint[f]
82	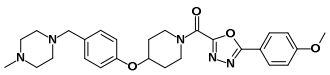	70	42[g]	ND	15	2.5 (2.0)	8.5	56 (0.29)	S
83	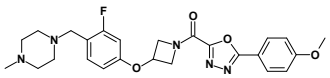	40	25[g]	#	>33	2.2 (2.7)	8.4	46 (0.35)	36
84	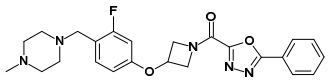	93	ND	ND	>33	2.1 (2.8)	8.4	46 (0.35)	20
85	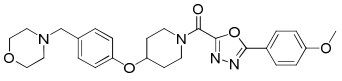	71	40[g]	ND	16	3.9 (1.5)	6.5	56 (0.29)	72

86	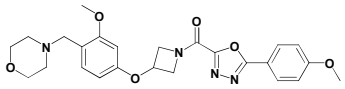	27	16[g]	ND	9.8	3.3 (2.1)	7.5	51 (0.47)	332
87	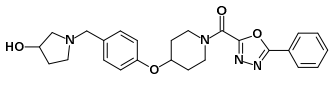	50	ND	>100	31	1.9 (1.0)	8.9	31 (0.9)	S
88	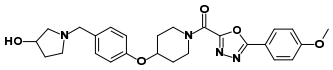	26	39[g]	293[h]	24	2 (1.0)	8.9	36 (0.63)	S
89	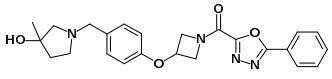	22	6	146	>33	1.45 (1.9)	9.0	34 (0.26)	S
90	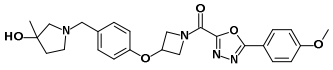	23	9	35	26	1.6 (2.0)	9.0	42 (0.78)	2.8
91	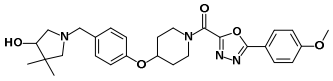	25	39[g]	91[h]	10	2.6 (2.0)	8.9	34 (0.26)	19

[a] Functional potency.[23] [b] RO receptor occupancy. IC_{50} relates to free plasma levels. [c] $LogD_{7.4}$ hplc [d] Experimental pKa[36] [e] 10^{-6} cm/s [f] µl/min/mg [g] Human binding data [h] Human plasma protein binding used to calculate IC_{50} RO, free. ND Not determined S Stable to assay conditions (100% parent compound remaining after incubation) # No EC50 curve was generated for this compound (**83**): 90% RO free @ 688 nM.

established, it was hypothesized that a logD below 2.5 should be targeted for metabolic stability and that a pKa below 9 would combine acceptable MCHr1 potency with reduced hERG interactions. Since introduction of a single HBD had a detrimental effect on RO pointing towards efflux and leading to poor CNS exposure, an additional design criterion was established to not incorporate an HBD. A set of compounds designed along these criteria are shown in **Table 6**. As design parameters, clogP and pKa were considered separately, rather than calculating a

composite logD. Certainly, a direct comparison between measured logD and the rather artificial clogP was not expected to correlate perfectly, nevertheless measured lipophilicity was markedly higher for the open oxetanes derivatives **95** and **96** despite good agreement between calculated and measured pKa. In line with earlier observations, metabolic turnover numbers for **95** and **96**

Table 6. Western modifications: spiro compounds and analogues

Compound	Structure	IC_{50} MCH $GTP\gamma S$[a] (nM)	IC_{50} MCH bind Mu (nM)	IC_{50} RO, free[b] (nM)	IC_{50} hERG (μM)	logD[c] (clogP)	pKa exp[d] (pKa calc)	Caco AB[e] (Efflux ratio)	HLM Clint[f]
94	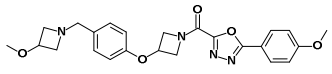	19	ND	ND	8.5	2.3 (2.5)	8.5 (7.8)	27[h]	51
95	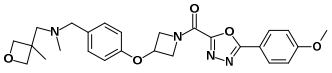	30	9	90% @ 0.5 nM[g]	16	4.1 (1.7)	8.0 (8.0)	21[h]	110
96	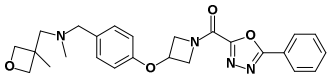	35	14	ND	14	4 (1.7)	8.5 (8.2)	24[h]	117
97	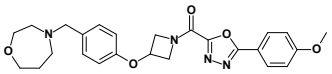	34	11	ND	25	2.4 (2.0)	8.1 (8.0)	51 (0.34)	37
98	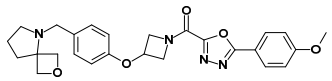	45	15	35% @ 5nM[g]	12	3.9 (2.3)	6.0 (7.9)	24[h]	74
99	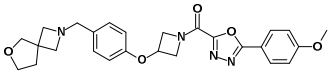	20	7	2	16	2.2 (2.1)	8.6 (8.6)	60 (0.3)	14
100	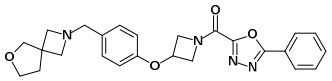	20	7	ND	16	2.1 (2.0)	8.6 (8.6)	22[h]	2
101	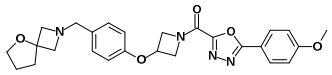	16	3	2	13	2.7 (2.3)	8.4 (7.7)	41 (0.3)	29

102	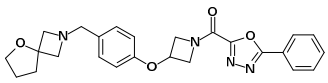	20	7	ND	8.9	2.6 (2.2)	8.4 (7.7)	31[h]	6
103	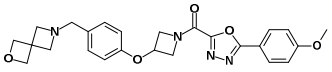	27	11	4	22	2.0 (2.1)	8.2 (8.0)	61 (0.46)	13
104	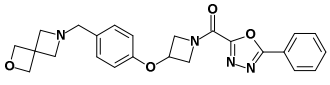	23	11	15	28	1.8 (2.1)	8.0 (8.0)	79 (0.26)	S

[a] Functional potency.[23] [b] RO receptor occupancy. IC_{50} relates to free plasma levels. [c] $LogD_{7.4}$ hplc [d] Experimental pKa[36] [e] 10^{-6} cm/s [f] µl/min/mg [g] Incomplete curves [h] Calculated values.[37] Probability of efflux were low for all these compounds. S Stable to assay conditions (100% parent compound remaining after incubation) ND Not determined

were high. The homomorpholine derivative **97** did offer an improvement in properties over morpholines, but metabolic turnover rate was still too high. Our primary attention was turned to spirocyclic amines as substituents in the western part of the molecule. Spirocyclic building blocks have seen an increasing interest in the literature recently.[38] For the 6-oxa-2-azaspiro[3.4]octanes (**99** and **100**) and the 2-oxa-6-azaspiro[3.3]heptanes (**103** and **104**), the measured pKa values mirrored well the predicted values and, also, measured lipophilicity was in agreement with clogP. It was pleasing to see the targeted physicochemical properties translated into improved metabolic stability coupled with a wider MCHr1 potency margin over the hERG channel. For other spirocycles, such as 2-oxa-5-azaspiro[3.4]octane (**98)** and 5-oxa-2-azaspiro[3.4]octanes (**101** and **102**) the measured physicochemical properties were more distant from the predicted values. None of these compounds showed sufficiently improved metabolic stability combined with an increased margin to hERG. It was also interesting to note that structurally related open ring analogues such as **95** and **96** were markedly more lipophilic for a

given pKa value and in none of these compounds could metabolic stability be combined with an increased margin over hERG potency. Although the metabolic turnover rate was somewhat higher for **99** and **103** than for the des-methoxy analogues **100** and **104**, the major metabolic route was shifted from the spirocycle to demethylation of the methoxy substituent in the eastern region of the molecules. It was speculated that metabolism in the strained spirocycle could be associated with formation of reactive metabolites and it was considered advantageous to direct metabolism to other parts of the molecule. A more detailed account of metabolite identification and metabolism pathways in the strained spirocyclic compounds is in preparation and will be reported. Turning to CNS properties, RO IC_{50} values for these spirocyclic amines suggested good target coverage in the CNS. Mouse binding data *in vitro* confirmed the potency observed in the RO assay, indicating a lack of efflux. In general, brain/plasma ratios were not measured in this program. The majority of compounds tested in the receptor occupancy model showed good agreement between *in vivo* and *in vitro* binding. Due to this correlation, *in vitro* potency could confidently be used to select compounds for testing in the DIO mouse model. Large deviations from the *in vitro-in vivo* correlation were attributed to efflux at the blood-brain barrier, presence of active metabolites or slow off-rate from the receptor *in vivo*. For example, compounds **80** and **95** displayed a markedly higher potency in the RO assay. The major metabolic pathway for these were demethylation of the eastern methoxy substituent leading to loss of MCHr1 potency, which speaks against active metabolites and suggests slow off-rate of the parent compounds *in vivo*. This shift towards higher potency was consistent for a small number of compounds, but this has not been confirmed in binding kinetics *in vitro*.

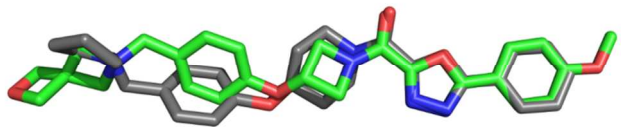

Figure 2. Structural overlay of X-ray structure of **103** (green carbons) in comparison with the low energy conformation of **1** (gray carbons) used as 3D-hypothesis for SAR analysis.

At this stage, the X-ray structure of compound **103** was solved (Supplementary information). Interestingly, this low energy conformation was in relatively good agreement with our 3D hypothesis, described by an elongated structure with overlapping pharmacophore elements (**Figure 2**). Although neither of these structures may be treated as the "true" bioactive conformation, the 3D information served as a good basis for further idea generation and interpretation of the SAR observed.

The results from the initial *ex vivo* receptor occupancy experiments were used to guide the dose setting in 3 week DIO mice studies. For most compounds in the series, a *bid* dosing regime was needed to keep the RO above a significant level for 24 hours. During the chemistry program, a trough RO of 70% was aimed for as a working hypothesis. At the end of the study, brain MCHr1 RO was determined *ex vivo* by autoradiography using the RO screening protocol. RO measurements at other time points were used together with plasma exposure profiles to model the RO over time. On the basis of the overall promising profile of **103**, this compound was further evaluated in a repeated dose DIO study in mice over 21 days. Based on the RO data, three different doses were selected aiming for a spread in RO profile. The aim was to vary the trough RO that would translate into different degrees of weight loss. In the DIO study, **103** was found to give a robust decrease in body weight when administered 50 or 20 μmol/kg twice daily *via* oral

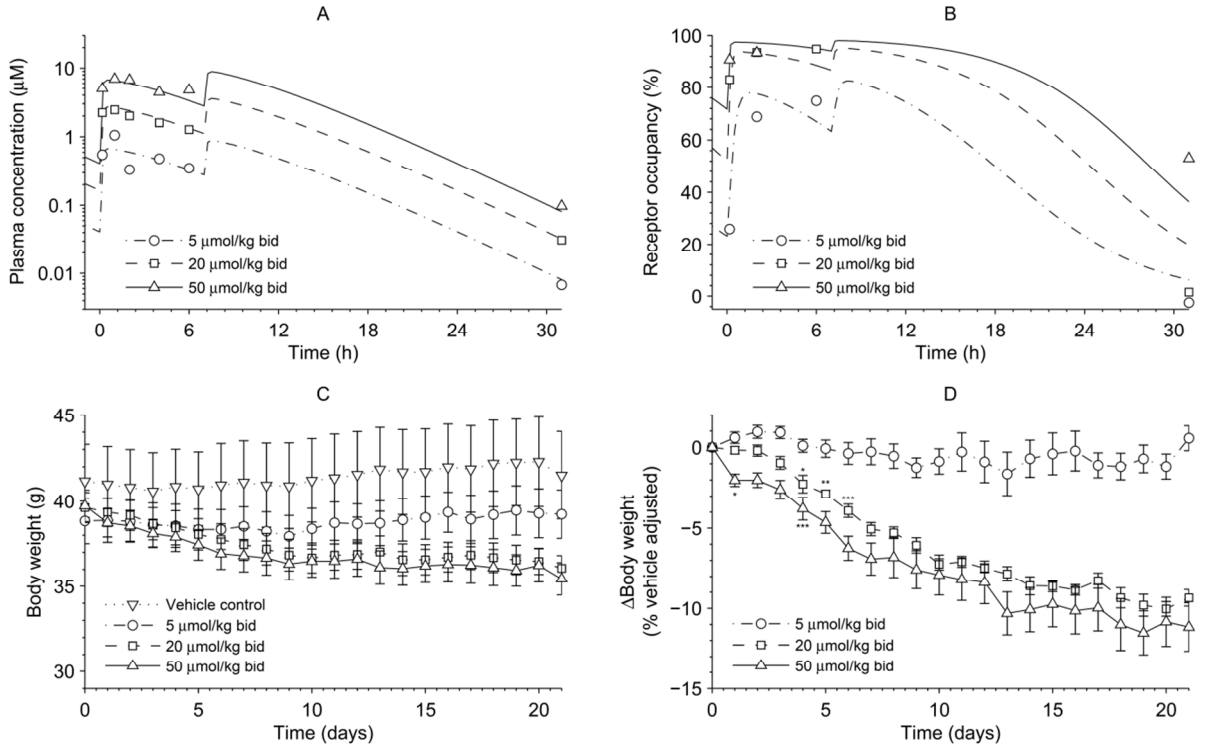

Figure 3. Effects of 103 on body weight in diet-induced obese mice.

Group housed female C57BL/6J mice were given free access to a cafeteria diet and randomized into experimental groups based on cage-average body weights and dosed with **103** (5, 20 or 50 μmol/kg bid at 8 am and 3 pm) or vehicle *via* oral gavage for 20 days. **A**) Plasma-exposure observations on the last study day and two-compartment pharmacokinetic model fit (k_a=0.27 h^{-1}, Cl=1.1 L/h/kg, V_1=0.25 L/kg, Q=0.92 L/h/kg, V_2=1.8 L/kg; relative bioavailability 1.7 for the 5 μmol/kg group and 1 for the other groups). **B**) Receptor-occupancy observations on the last study day and fits of a receptor-kinetic model with elementary reactions that was driven by the plasma concentration (K_D=0.18 μM, k_{off} =0.68 h^{-1}, R_{tot} =100). Effects on (**C**) body weight and (**D**) percentage vehicle adjusted body weight change (n = 5-6 per group). Data represent mean ± s.e.m. *P<0.05, **P<0.01, ***P<0.001 onwards *vs*. vehicle, one sided t-tests.

gavage, while 5 μmol/kg twice daily had a minor effect compared to vehicle dosed DIO mice (**Figure 3**). Thus, RO 24 hours after the first dose represents the trough value. For the two higher doses of **103**, trough RO levels were high enough to adequately inhibit MCHr1. It has been established in other studies that **103** had no effect on food intake or body weight in DIO mice lacking the MCHr1. These results confirmed that the observed weight loss was connected to the MCHr1 mechanism and not an effect related to taste of the drug or some toxic effect. Thus, **103** binds to MCHr1 in the brain and produces a RO driven body weight loss in DIO mice. The RO is driven in a predictable way by free plasma exposure, as **103** is not a Pgp substrate and shows no signs of efflux.

Compound **103** was extensively profiled from a DMPK, off target and safety pharmacology perspective. Additional pharmacokinetic data are summarized in **Table 7**. For this compound, and for the series in general, there was a good correlation between *in vitro* and *in vivo* clearance. No reversible or time dependent CYP450 inhibition was observed and *in vitro* safety pharmacology from broad panel screening was considered to be low risk.[39] There was no evidence of reactive metabolite formation from GSH or KCN trapping studies in HLM.

Table 7. Pharmacokinetic properties of 103.

Species	Hepatocyte CL_{int}[a]	Ppb[b] (% free)	CL[c]	V_{ss} (L/kg)	$t_{½}$ (h)	F (%)
Rat	5	10	9	2.0	1.8	92
Dog	24	36	37	5.4	1.7	18
Human	11	26	NA	NA	NA	NA

[a] µl/min/10^6 cells [b] plasma protein binding [c] ml/min/kg NA Not applicable

Additionally, **103** was inactive in an MCHr2 binding assay. Cardiovascular safety studies *in vivo* in either anaesthetized guinea pigs or dogs equipped with a telemetry system did not produce any noticeable treatment related effects on blood pressure, heart rate or QT up to a free plasma concentration of 3µM. Subsequently, compound **103** was evaluated in one month rat and dog GLP safety studies without any treatment related findings up to a dose of 100 mg/kg. The margins established in these studies together with the rest of the preclinical data package gave support for progression of **103**[40] into clinical studies, but the study was terminated after the study stopping criteria were reached.[41] Results from these clinical trials, as well as detailed accounts of human PK and the basis for dose setting in these studies will be disclosed in future publications.

Conclusion

Lead optimization on a series of novel MCHr1 antagonists resulted in the discovery of the clinical candidate **103**. The lead series fits well into the MCHr1 pharmacophore model, but occupies a markedly different physicochemical property space with reduced lipophilicity as compared to other published MCHr1 antagonists. The starting point **1** displayed favourable physicochemical properties and a clear focus throughout the chemistry program was to further reduce lipophilicity whilst retaining CNS properties and MCHr1 RO in the brain.

The use of an *ex vivo* RO model in mice was the key to providing fast and high quality data. In addition to ranking between compounds, the RO assay was also used to set doses for *in vivo* disease model studies, as well as guiding subsequent rounds of compound design. The candidate compound **103** has excellent DMPK properties and gave robust effects on weight loss when

dosed orally in a DIO mouse model. Preclinical GLP tox and safety pharmacology studies were without treatment related findings and **103** was selected as a clinical candidate.

EXPERIMENTAL SECTION

Complete experimental information can be found in Supporting Information. ^{1}H NMR spectra were recorded at 300, 400, 500 or 600 MHz. Chemical shifts (ppm) were determined relative to internal solvent (^{1}H, δ 7.24 ppm; $CDCl_3$, δ 2.50 ppm; DMSO-d_6, δ 3.31 ppm; methanol-d_4). Analytical HPLC/MS was conducted on a QTOF mass spectrometer using a UV detector monitoring either at (a) 210 nm with a BEH C18 column (2.1mm × 100 mm, 1.7 μm, 0.7 mL/min flow rate), using a gradient of 2% v/v CH_3CN in H_2O (ammonium carbonate buffer, pH 10) to 98% v/v CH_3CN in H_2O, or at (b) 230 nm with an HSS C18 column (2.1 × 100 mm, 1.8 μm, 0.7 mL/min flow rate), using a gradient of 2% v/v CH_3CN in H_2O (ammonium formate buffer, pH 3) to 98% v/v CH_3CN in H_2O. All tested compounds with one exception (compound **91**, 93% pure) were determined to be ≥95% pure using the analytical method a or b described above based on the peak area percentage. High-resolution mass spectra were carried out using high-resolution electrospray ionization mass spectrometry (HRESIMS) where the spectrometer was linked together with an Aquity®UPLC system.

The following 5-phenyl-1,3,4-oxadiazole intermediates were synthesized from the corresponding benzohydrazides in a similar fashion to that described by Dost[42] and co-workers: Ethyl 5-(4-chlorophenyl)-1,3,4-oxadiazole-2-carboxylate, ethyl 5-(4-methoxyphenyl)-1,3,4-oxadiazole-2-carboxylate, ethyl 5-phenyl-1,3,4-oxadiazole-2-carboxylate, 5-[4-(difluoro-methoxy)phenyl]-1,3,4-oxadiazole-2-carboxylate, ethyl 5-(4-fluorophenyl)-1,3,4-oxadiazole-2-carboxylate and

ethyl 5-(2-chlorophenyl)-1,3,4-oxadiazole-2-carboxylate. Unless stated, all other reagents and solvents were used as purchased without purification.

Synthetic procedures to 103.

Reductive amination as the final step:

(3-Hydroxyazetidin-1-yl)(5-(4-methoxy-phenyl)-1,3,4-oxadiazol-2-yl)methanone (52).

To a stirred suspension of 5-(4-methoxyphenyl)-1,3,4-oxadiazole-2-carboxylate (9.00 g, 36.3 mmol) in dry MeOH (135 mL) was added sodium cyanide (0.35 g, 7.3 mmol). A solution of 3-hydroxyazetidinium chloride (6.21 g, 45.3 mmol) and triethylamine (6.3 mL, 45.3 mmol) in MeOH (45 mL) was added and the mixture was stirred at ambient temperature for 2 h. Water (135 mL) was added together with DCM (135 mL). After mixing and separation of the two layers, the aqueous phase was extracted twice with DCM. The combined organic solutions were concentrated to dryness under reduced pressure. The solid residue was slurried in toluene (45 mL) and then filtered. The filter cake was washed twice with water (45 ml). Drying overnight in vacuum at 40°C afforded the desired **52** as a white solid (7.7 g, 77%). ^{1}H NMR (500 MHz, DMSO-d_6) δ 7.97 (d, J = 8.9 Hz, 2H), 7.15 (d, J = 8.9 Hz, 2H), 5.86 (d, J = 6.4 Hz, 1H), 4.71-4.80 (m, 1H), 4.50-4.60 (m, 1H), 4.23-4.35 (m, 2H), 3.78-3.88 (m, 4H). MS m/z 276 $[M+H]^+$.

1-(5-(4-Methoxyphenyl)-1,3,4-oxadiazole-2-carbonyl)azetidin-3-yl methane-sulfonate (53).

To an ice- cooled mixture of **52** (6.1 g, 22.2 mmol) and triethylamine (4.3 mL, 31.0 mmol) in DCM (150 ml) was dropwise added methanesulfonyl chloride (2.4 mL, 31.0 mmol). After stirring at 0°C for 1.5 h, the mixture was allowed to warm to room temperature and was then stirred overnight at ambient temperature. The solution was washed with water and then with a

saturated solution of $NaHCO_3$. The organic layer was dried using a phase separator and then evaporated to dryness to afford **53** as a solid (6.03 g, 77%). ^{1}H NMR (500 MHz, $CDCl_3$) δ 8.09 (d, J = 8.7 Hz, 2H), 7.02 (d, J = 8.7 Hz, 2H), 5.36-5.43 (m, 1H), 5.07-5.14 (m, 1H), 4.82-4.90 (m, 1H), 4.60-4.67 (m, 1H), 4.37-4.44 (m, 1H), 3.89 (s, 3H), 3.12 (s, 3H). MS m/z 354 $[M+H]^+$.

4-(1-(5-(4-Methoxyphenyl)-1,3,4-oxadiazole-2-carbonyl)azetidin-3-yloxy)benzaldehyde (54).

A mixture of **53** (6.0 g, 17.0 mmol), 4-hydroxybenzaldehyde (2.28 g, 18.7 mmol) and cesium carbonate (6.09 g, 18.7 mmol) in DMA (100 mL) was heated at 110°C overnight. The mixture was allowed to warm to room temperature and then partitioned between water and DCM. The organic solution was washed with water and then dried using a phase separator. The solvent was removed by evaporation and to the residue was added diethyl ether. The formed solid was isolated by filtration. The filter cake was washed with diethyl ether and then dried under reduced pressure to give **54** as a beige solid (4.8 g, 75%). ^{1}H NMR (500 MHz, $CDCl_3$) δ .9.92 (s, 1H), 8.10 (d, J = 8.8 Hz, 2H), 7.88 (d, J = 8.8 Hz, 2H), 7.03 (d, 8.8 Hz, 2H), 6.91 (d, J = 8.8 Hz, 2H), 5.13-5.52 (m, 2H), 4.75-4.83 (m, 1H), 4.66-4.73 (m, 1H), 4.32-4.39 (m, 1H), 3.89 (s, 3H). MS m/z 380 $[M+H]^+$.

(3-(4-(2-Oxa-6-azaspiro[3.3]heptan-6-ylmethyl)phenoxy)azetidin-1-yl)(5-(4-methoxyphenyl)-1,3,4-oxadiazol-2-yl)-methanone (103).

To a stirred suspension of **54** (2.49 g, 6.57 mmol) and 2-oxa-6-azaspiro-[3.3]heptane[38b] (1.31 g, 7.31 mmol) in DCM (25 mL) was added triethylamine (2.8 mL, 20.1 mmol). The mixture was cooled by an ice-bath and then sodium triacetoxy-borohydride (2.15 g, 10.1 mmol) was added in small portions during 45 min. After allowing the mixture to warm to room temperature, a further portion of sodium triacetoxyborohydride (0.42 g, 1.98 mmol) was added. Stirring was continued

overnight and water (20 mL) was then slowly added. The layers were separated and the aqueous phase was washed with DCM. The combined organic solutions were washed with brine and concentrated to afford a mixture of an oil and an aqueous phase. The aqueous layer was discarded and the oily residue was co-evaporated with EtOH, and then dissolved in DCM. The solution was washed with an aqueous $NaHCO_3$ solution and then concentrated. Again, an aqueous layer was discarded and the oily residue was partitioned between DCM and an aqueous solution of Na_2CO_3. The layers were separated using a phase separator and the organic solution was evaporated. The residue was treated with methyl *tert*-butyl ether to give a beige solid that was isolated by filtration. The filter cake was washed with *tert*-butyl ether and dried in the hood overnight to afforded **103** (1.90, 62%) as a beige solid. ^{1}H NMR (400 MHz, DMSO-d_6): δ 7.99 (d, J = 9.07 Hz, 2H), 7.12-7.20 (m, 4H), 6.80 (d, J = 8.6 Hz, 2H), 4.98-5.18 (m, 2H), 4.43-4.64 (m, 6H), 3.99-4.10 (m, 1H), 3.85 (s, 3H), 3.39 (s, 2H), 3.22 (s, 4H). HRESIMS calcd for $C_{25}H_{26}N_4O_5^+$ $(M)^+$, 463.1981; found 463.1950.

Amide formation as the final step:

4-(2-Oxa-6-azaspiro[3.3]hept-6-ylmethyl)phenol (35).

To a stirred solution of 4-hydroxybenzaldehyde (0.85 g, 6.94 mmol) in DCM (35 mL) was added 2-oxa-6-azaspiro[3.3]heptane[38b] 1.00 g, 6.94 mmol). After stirring for 20 min, sodium triacetoxyborohydride (1.91 g, 9.02 mmol) was added and the reaction mixture was stirred overnight. Another portion of 2-oxa-6-azaspiro[3.3]heptane (0.10 g, 0.69 mmol) was added, stirring was continued for 2 h and then further sodium triacetoxy-borohydride (0.30 g, 1.42 mmol) was added. The mixture was stirred for additionally 2 h and then DCM and water were added. After the organic layer was removed, the aqueous phase was carefully basified with small

portions of K_2CO_3. The solution was extracted several times with DCM and the combined organic solutions were dried using a phase separator. The solvent was removed by evaporation to afford **35** (1.20 g, 84%) as an oil. ^{1}H NMR (500 MHz, $CDCl_3$) δ 7.04 (d, J = 8.4 Hz, 2H), 6.61 (d, J = 8.4 Hz, 2H), 4.72 (s, 4H), 3.48 (s, 2H), 3.42 (s, 4H). MS m/z 206 $[M+H]^+$.

***tert*-Butyl 3-[4-(2-oxa-6-azaspiro[3.3]hept-6-ylmethyl)phenoxy]azetidine-1-carboxylate (36).**

To a solution of **35** (0.77 g, 3.75 mmol) in DMF (20 mL) was added cesium carbonate (2.45 g, 7.50 mmol). After stirring for 10 min, *tert*-butyl 3-(methylsulfonyl-oxy)azetidine-1-carboxylate (2.45 g, 7.50 mmol) was added. The reaction mixture was stirred at 90 °C for 24 h and then allowed to warm to room temperature. After filtration, the mixture was filtered and the filtrate was evaporated. The product was purified by reverse phase HPLC using a gradient of MeCN (15% → 55%) in 0.2% ammonia buffer as eluent. There was obtained an oil of **36** (1.00 g, 74%) which solidified on standing. ^{1}H NMR (500 MHz, $CDCl_3$) δ 7.15 (d, J = 8.5 Hz, 2H), 6.68 (d, J = 8.5 Hz, 2H), 4.78-4.90 (s, 3H), 4.73 (s, 4H), 4.28 (dd, J = 9.5, 6.7 Hz, 1H), 3.99 (dd, J = 9.5, 4.1 Hz, 1H), 3.46 (s, 2H), 3.34 (s, 4H), 1.45 (s, 9H). MS m/z 361 $[M+H]^+$.

6-(4-(Azetidin-3-yloxy)benzyl)-2-oxa-6-azaspiro[3.3]heptane (37).

36 (1.00 g, 2.77 mmol) was dissolved in DCM (100 mL) and then TFA (10 mL) was added. The reaction mixture was stirred at ambient temperature for 1 h. Solid K_2CO_3 (23 g) was added in small portions and the mixture was stirred for 1 h. A saturated aqueous solution of K_2CO_3 was added and after mixing, the layers were separated. The aqueous solution was extracted 5 times with DCM. The combined organic solutions were dried using a phase separator and then evaporated to give **37** (0.60 g, 83%) as a colorless oil. ^{1}H NMR (500 MHz, $CDCl_3$) δ 7.13 (d, J =

8.7 Hz, 2H), 6.69 (d, *J* = 8.7 Hz, 2H), 4.93-5.00 (m, 1H), 4.73 (s, 4H), 3.88-3.95 (m, 2H), 3.75-3.82 (m, 2H), 3.45 (s, 2H), 3.34 (s, 4H). MS m/z 261 $[M+H]^+$.

(3-(4-(2-Oxa-6-azaspiro[3.3]heptan-6-ylmethyl)phenoxy)azetidin-1-yl)(5-(4-methoxyphenyl)-1,3,4-oxadiazol-2-yl)-methanone (103).

To a solution of **37** (0.45 g, 1.7 mmol) in MeOH (20 ml) was added ethyl 5-(4-methoxyphenyl)-1,3,4-oxadiazole-2-carboxylate (0.47 g, 1.9 mmol) and sodium cyanide (17 mg, 0.35 mmol). The mixture was stirred at ambient temperature for 2 h and then the volatiles were removed under reduced pressure. The product was purified by column chromatography on silica gel. Elution with a gradient of NH_3/MeOH (2M) in DCM (1% → 3%) provided **103** (0.52 g, 65%) as solid. ^{1}H NMR (400 MHz, $CDCl_3$): δ 8.08 (d, *J* = 9.0 Hz, 2H), 7.17 (d, *J* = 8.7 Hz, 2H), 7.01 (d, *J* = 9.0 Hz, 2H), 6.72 (d, *J* = 8.7 Hz, 2H), 5.00-5.14 (m, 2H), 4.69-4.76 (m, 5H), 4.58-4.66 (m, 1H), 4.27-4.34 (m, 1H), 3.88 (s, 3H), 3.47 (s, 2H), 3.35 (s, 4H). HRESIMS calcd for $C_{25}H_{26}N_4O_5^+$ $(M)^+$, 463.1981; found 463.1959.

Biological assays

***Ex vivo* brain Mchr1 occupancy in mice**

Animal Treatments

Female C57Bl/6J mice had access to either cafeteria diet and/or standard chow (R3) for several weeks before the start of treatment with compound. Mice (n=2-3/group) were weighed and then single dosed with compound. They were sacrificed after different time points up to 24 h post dose. Brains are taken out and freezed on dry ice. Orbital blood was collected for later exposure analysis. Plasma samples and brains were thereafter stored at –80 C°.

Ex vivo autoradiographic binding

Sectioning

20 μm coronal brain sections were cut from caudate putamen (Mchr1), in a cryostat at –15°C and thawmounted on SuperFrost®Plus glasses (Menzel-Glaser, Braunschweig, Germany), 3 sections per slide. These were stored at -80°C until use (max 3 months).

Ex vivo binding (Mchr1)

Slides were allowed to warm to room temperature in a stream of air. The sections were incubated at room temperature in 50mM Tris-HCl, 10mM $MgCl_2$, 0.16mM PMSF, 1mM Phenantroline, 100 μM Dopamine, 1 μM Prazosin, 0.2% BSA and 0.3 nM [^{3}H]-SNAP-7941[43] at pH 7.4 for 10 min at room temperature. Non-specific slides were incubated in above solution containing 10 μM 4-(2-((4α*S*,11*S*,11α*R*)-11-methyl-9-(trifluoromethyl)-3,4,4α,5-tetrahydro-1*H*-pyrido[4,3-b]carbazol-2(6*H*,11*H*,11α*H*)-yl)ethyl)morpholine (Compound **9** in the referenced paper).[12a] Following incubation with radioligand, the slides were rinsed in 50 mM ice-cold Tris-HCl, pH 7.4 for 3 x 2 min, dipped in ice cold distilled water 2 x 15 seconds to remove salts and then quickly dried using a fan. (K_D for [^{3}H]-SNAP-7941 in mouse brain striatum 0.225 nM)

Imaging

Before exposure of the slides, the imaging plates (BAS IP-TR 2025 Tritium imaging plates) were erased for30 min in IP eraser.

The sections were placed in a hypercassette and exposed for 4 days to imaging plates with [^{3}H] microscales (Amersham Biosciences UK) as standard. The cassette cover was closed to start exposure and the cassette put in a lead Shielding Box.

After complete exposure, the cassette was opened under subdued light and the imaging plate was placed in the IP-reader BAS-5000 Bio-Imaging Analyzer (Fuji Photo Film,Tokyo Japan) and scanned.

Data analysis

Quantification was made using an image analyzer software (Fuji Film, Science lab, Multi Gauge 3.1 and 3.2).in order to measure optical densities in caudate putamen (MCHR). Specific *in vivo* occupancy calculation: 100-(dose-non-specific / vehicle-non-specific x100).A compound that occupied brain receptors >10% was reported as being active in the test system. Those compounds that induced <10% brain occupancy was reported as not active in the test system.

Body weight and *ex vivo* brain Mchr1 occupancy in DIO mice

The animal experiments were approved by the Gothenburg Ethics Committee for Experimental Animals in Sweden.

Group housed eight weeks old female C57BL/6J mice were given free access to a cafeteria diet consisting of cheese (Västervik, Arla AB, Sweden), milk chocolate (Marabou AB, Sweden), chocolate confection (Delicato Bakverk AB, Huddinge, Sweden) and standard chow diet (R3, lactamin AB, Sweden) for 8 weeks at Harlan (Holland) prior to shipment to AstraZeneca. The mice were then kept in the same groups, fed the same diet and subjected to a reverse light-dark cycle (lights off at 10 am and on at 10 pm) throughout the study. Two weeks after arrival at AstraZeneca, the mice were randomized into experimental groups based on cage average body weights and dosed with **103** (5, 20 or 50 μmol/kg bid at 8 am and 3 pm) or vehicle via oral gavage for 20 days.

After the body weight study, the mice were dosed once more with the respective doses of **103** (5, 20 or 50 μmol/kg) and terminated after 10 min, 1 h, 2 h, 7 h, 8 h or 24 h. After death, brains were dissected, quickly frozen on dry ice and stored at -80°C before measurement of *ex vivo* brain Mchr1 occupancy analysis according to the procedure described above.

Data analyses

Data represent mean ± s.e.m. body weight changes and were analyzed using pair-wise one-sided *t*-tests *vs* the vehicle group and data was log transformed before the analysis.

DMPK and safety pharmacology assays, including hERG

All DMPK and safety pharmacology assays have been described earlier.[36, 44]

ASSOCIATED CONTENT

Supporting information

Detailed synthetic chemistry procedures, description of computational chemistry methods used, X-ray diffraction data and full description *of in vitro* and *in vivo* biological methods.

ABBREVIATIONS USED

CV, cardiovascular; DIAD, diisopropyl azodicarboxylate; DIO, Diet Induced Obesity; H3, histamine 3; HLM, human liver microsomes; hERG, human ether-à-go-go-related gene; LLE, lipophilic ligand efficiency; MCHr1, Melanin Concentrating Hormone receptor 1; MCHr2, Melanin Concentrating Hormone receptor 2; RLM, rat liver microsomes; RO, Receptor Occupancy; TEA, triethyl amine

AUTHOR INFORMATION

Corresponding Author

*E-mail: anders.m.johansson@astrazeneca.com. Phone: +46317762822.

Notes

The authors declare no competing financial interest.

Present Addresses

†If an author's address is different than the one given in the affiliation line, this information may be included here.

ACKNOWLEDGEMENT

We wish to thank staff at the CVMD Bioscience department, the Laboratory Animal Sciences staff as well as staff at Discovery Sciences at AstraZeneca Gothenburg for assisting with these studies. We acknowledge Jeffrey Albert, Jennifer Krumrine, Rebecca Urbanek and Vijaya Tiranugaru all formerly of AstraZeneca, Wilmington for a good collaboration in the initial stages of the program. We also thank Janet M. Forst and Gary B. Steelman, both formerly of AstraZeneca, Wilmington and Marika Lindhagen, AstraZeneca Gothenburg for assistance in preparation of compounds **1** and **103** and Chad Elmore and Cecilia Eriksson, AstraZeneca Gothenburg for preparation of [^{3}H]-SNAP-7941.

REFERENCES

1. a) Colman, E. Food and drug administration's obesity drug guidance document: a short history. *Circulation* **2012**, *125*, 2156-2164. b) Guh, D. P.; Zhang, W.; Bansback, N.; Amarsi, Z.;

Birmingham, C. L.; Anis, A. H. The incidence of co-morbidities related to obesity and overweight: a systematic review and meta-analysis. *BMC Public Health* **2009**, *9*, 88. c) Malik, V. S.; Willett, W. C.; Hu, F. B. Global obesity: trends, risk factors and policy implications. *Nat. Rev. Endocrinol.* **2013**, *9*, 13-27.

2. Gouni-Berthold, I.; Bruning, J. C.; Berthold, H. K. Novel approaches to the pharmacotherapy of obesity. *Curr. Pharm. Des.* **2013**, *19*, 4938-4952.

3. Sargent, B. J.; Moore, N. A. New central targets for the treatment of obesity. *Br. J. Clin. Pharmacol.* **2009**, *68*, 852-860.

4. Takase , K.; Kikuchi, K.; Tsuneoka, Y.; Oda, S.; Kuroda, M.; Funato, H. Meta-analysis of melanin-concentrating hormone signaling-deficient mice on behavioral and metabolic phenotypes. *PLOS One.* **2014**, *9*, e99961.

5. a) Kilduff, T. S.; de Lecea, L. Mapping of the mRNAs for the hypocretin/orexin and melanin-concentrating hormone receptors: networks of overlapping peptide systems. *J. Comp. Neur.* **2001**, *435*, 1-5. b) Hervieu, G. J.; Cluderay, J. E.; Harrison, D.; Meakin, J.; Maycox, P.; Nasir, S.; Leslie, R. A. The distribution of the mRNA and protein products of themelanin-concentrating hormone (MCH) receptor gene, SLC-1, in the central nervous system of the rat. *Eur. J. Neurosci.* **2000**, *12*, 1194-1216.

6. Shimada, M.; Tritos, N. A.; Lowell, B. B.; Flier, J. S.; Maratos-Flier, E. Mice lacking melanin-concentrating hormone are hypophagic and lean. *Nature (London)* **1998**, *396*, 670-674.

7. a) Astrand, A.; Bohloody, M.; Larsdotter, S.; Mahlapuu, M.; Andersén, H.; Tornell, J.; Ohlsson, C.; Snaith, M.; Morgan, D. G. A. Mice lacking melanin-concentrating hormone receptor 1 demonstrate increased heart rate associated with altered autonomic activity. *Am. J. Physiol. Regul. Integr. Comp. Physiol.* **2004**, *287*, R749-R758. b) Marsh, D. J.; Weingarth, D. T.;

Novi, D. E.; Chen, H. Y.; Trumbauer, M. E.; Chen, A. S.; Guan, X. M.; Jiang, M. M.; Feng, Y.; Camacho, R. E.; Shen, Z.; Frazier, E. G.; Yu, H.; Metzger, J. M.; Kuca, S. J.; Shearman, L. P.; Gopal-Truter, S.; MacNeil, D. J.; Strack, A. M.; MacIntyre, D. E.; Van der Ploeg, L. H.; Qian, S. Melanin-concentrating hormone 1 receptor-deficient mice are lean, hyperactive, and hyperphagic and have altered metabolism. *Proc. Natl. Acad. Sci. U S A.* **2002**, *99*, 3240-3245.

8. Ito, M.; Ishihara, A.; Gomori, A.; Matsushita, H.; Ito, M.; Metzger, J. M.; Marsh, D. J.; Haga, Y.; Iwaasa, H.; Tokita, S.; Takenaga, N.; Sato, N.; MacNeil, D. J.; Moriya, M.; Kanatani, A. Mechanism of the anti-obesity effects induced by a novel melanin-concentrating hormone 1-receptor antagonist in mice. *Br. J. Pharmacol.* **2010**, *159*, 374-383.

9. a) Goldstein, C.; Schroeder, J. C.; Fortin, J.-P.; Goss, J. M.; Schaus, S. E.; Beinborn, M.; Kopin, A. S. Two naturally occurring mutations in the type 1 melanin-concentrating hormone receptor abolish agonist-induced signaling. *J. Pharmacol. Exp. Ther.* **2010**, *335*, 799-806. b) Macneil, D. J. The role of melanin-concentrating hormone and its receptors in energy homeostasis. *Front. Endocrinol. (Lausanne).* **2013**, *4*, 49.

10. Tan, C. P.; Sano, H.; Iwaasa, H.; Pan, J.; Sailer, A. W.; Hreniuk, D. L.; Feighner, S. D.; Palyha, O. C.; Pong, S.-S.; Figueroa, D. J.; Austin, C. P.; Jiang, M. M.; Yu, H.; Ito, J.; Ito, M.; Ito, M.; Guan, X. M.; MacNeil, D. J.; Kanatani, A.; Van der Ploeg, L. H. T.; Howard, A. D. Melanin-concentrating hormone receptor subtypes 1 and 2: species-specific gene expression. *Genomics* **2002**, *79*, 785-792.

11. Chee, M. J.; Pissios, P.; Prasad, D.; Maratos-Flier, E. Expression of melanin-concentrating hormone receptor 2 protects against diet-induced obesity in male mice. *Endocrinology* **2014**, *155*, 81-88.

12. a) Mihalic, J. T.; Chen, X.; Fan, P.; Chen, X.; Fu, Y.; Liang, L.; Reed, M.; Tang, L.; Chen, J.-L.; Jaen, J.; Li, L.; Dai, K. Discovery of a novel series of melanin-concentrating hormone receptor 1 antagonists for the treatment of obesity. *Bioorg. Med. Chem. Lett.* **2011**, *21*, 7001-7005. b) Motani, A. S.; Luo, J.; Liang, L.; Mihalic, J. T.; Chen, X.; Tang, L.; Li, L.; Jaen, J.; Chen, J. L.; Dai, K. Evaluation of AMG 076, a potent and selective MCHR1 antagonist, in rodent and primate obesity models. *Pharmacol. Res. Perspect.* **2013**, *1*, e00003.

13. Chen, X.; Mihalic, J.; Fan, P.; Liang, L.; Lindstrom, M.; Wong, S.; Ye, Q.; Fu, Y.; Jaen, J.; Chen, J.-L.; Dai, K.; Li, L. Discovery and characterization of a potent and selective antagonist of melanin-concentrating hormone receptor 2. *Bioorg. Med. Chem. Lett.* **2012**, *22*, 363-366.

14. Shimazaki, T.; Yoshimizu, T.; Chaki, S. Melanin-concentrating hormone MCH1 receptor antagonists a potential new approach to the treatment of depression and anxiety disorders. *CNS Drugs* **2006**, *20*, 801.

15. Ito, M.; Gomori, A.; Suzuki, J.; Tsujioka, S.; Sasaki, M.; Matsuda, M.; Bednarek, M. A.; Ito, M.; Ishihara, A.; Iwaasa, H.; Macneil, D. J.; Kanatani, A. Antagonism of central melanin-concentrating hormone 1 receptor alleviates steatohepatitis in mice. *J. Endocrinol.* **2008**, *198*, 309-315.

16. Parks, G. S.; Okumura, S. M.; Gohil, K.; Civelli, O. Mice lacking Melanin Concentrating Hormone 1 receptor are resistant to seizures. *Neurosci. Lett.* **2010**, *484*, 104-107.

17. a) Johansson, A. Recent progress in the discovery of melanin-concentrating hormone 1-receptor antagonists. *Expert Opin. Ther. Pat.* **2011**, *21*, 905-925. b) Luthin, D. R. Anti-obesity effects of small molecule melanin-concentrating hormone receptor 1 (MCHR1) antagonists. *Life Sci.* **2007**, *81*, 423-440. c) Johansson, A.; Lofberg, C. Novel MCH1 receptor antagonists: a patent review. *Expert Opin. Ther. Pat.* **2015**, *25*, 193-207. d) Szalai, K. K.; Beke, G.; Eles, J.; Kitka, T.;

Kovacs, P.; Nagy, J.; Farkas, S.; Boros, A. Recent patents on novel MCH1 receptor antagonists as potential anti-obesity drugs. *Recent Pat. CNS Drug Discovery* **2014**, *9*, 122-140.

18. Hogberg, T.; Frimurer, T. M.; Sasmal, P. K. Melanin concentrating hormone receptor 1 (MCHR1) antagonists-Still a viable approach for obesity treatment? *Bioorg. Med. Chem. Lett.* **2012**, *22*, 6039-6047.

19. Bingham, M.; Rankovic, Z. Medicinal chemistry challenges in CNS drug discovery. *RSC Drug Discovery Ser.* **2012**, *28*, 465-509.

20. Moore, N. A.; Sargent, B. J.; Guzzo, P. R.; Surman, M. D. From preclinical to clinical development: the example of a novel treatment for obesity. *Neurobiol. Dis.* **2014**, *61*, 47-54.

21. a) Berglund, S.; Egner, B. J.; Graden, H.; Graden, J.; Morgan, D. G.; Inghardt, T.; Giordanetto, F. Optimization of 2-piperidin-4-yl-acetamides as melanin-concentrating hormone receptor 1 (MCH-R1) antagonists: Designing out hERG inhibition. *Bioorg. Med. Chem. Lett.*. **2009**, *19*, 4268-4273. b) Berglund, S.; Egner, B. J.; Graden, H.; Graden, J.; Morgan, D. G.; Inghardt, T.; Giordanetto, F. Optimization of piperidin-4-yl-urea-containing melanin-concentrating hormone receptor 1 (MCH-R1) antagonists: Reducing hERG-associated liabilities. *Bioorg. Med. Chem. Lett.*. **2009**, *19*, 4274-4279. c) Berglund, S.; Egner, B. J.; Graden, H.; Graden, J.; Morgan, D. G.; Inghardt, T.; Giordanetto, F. Discovery of 1,3-disubstituted-1H-pyrrole derivatives as potent melanin-concentrating hormone receptor 1 (MCH-R1) antagonists. *Bioorg. Med. Chem. Lett.*. **2008**, *18*, 4859-4863. d) Giordanetto, F.; Karlsson, O.; Lindberg, J.; Larsson, L. O.; Linusson, A.; Evertsson, E.; Morgan, D. G.; Inghardt, T. Discovery of cyclopentane- and cyclohexane-trans-1,3-diamines as potent melanin-concentrating hormone receptor 1 antagonists. *Bioorg. Med. Chem. Lett.*. **2007**, *17*, 4232-4241.

22. Thomsen, W.; Frazer, J.; Unett, D. Functional assays for screening GPCR targets. *Curr. Opin. Biotechnol.* **2005**, *16*, 655-665.

23. Harrison, C.; Traynor, J. R. The [35S]GTPγS binding assay: approaches and applications in pharmacology. *Life Sci.* **2003**, *74*, 489-508.

24. GOSTAR (GVK Bio Online Structure Activity Relationship Database. https://gostardb.com/gostar/ (Accessed September 12 2013)

25. For calculation of pKa and PSA, methods from ACD/labs® were used throughout the chemistry program. (Advanced Chemistry Development, Inc., Toronto, ON, Canada, www.acdlabs.com) Calculations of ClogP were made using ClogP version 4.3 (Pomona College and Biobyte Inc., Claremont, Calif. USA). These can be easily accessed through the internal C-lab portal: http://dalkescientific.com/writings/CLab-EuroQSAR2008.pdf

26. Philippe, C.; Haeusler, D.; Fuchshuber, F.; Spreitzer, H.; Viernstein, H.; Hacker, M.; Wadsak, W.; Mitterhauser, M. Comparative autoradiographic in vitro investigation of melanin concentrating hormone receptor 1 ligands in the central nervous system. *Eur. J. Pharmacol.* **2014**, *735*, 177-183.

27. a) Smith, D. G.; Hegde, L. G.; Wolinsky, T. D.; Miller, S.; Papp, M.; Ping, X.; Edwards, T.; Gerald, C. P.; Craig, D. A. The effects of stressful stimuli and hypothalamic-pituitary-adrenal axis activation are reversed by the melanin-concentrating hormone 1 receptor antagonist SNAP 94847 in rodents. *Behav. Brain Res.* **2009**, *197*, 284-291. b) Ito, M.; Sakamoto, T.; Suzuki, T.; Egashira, S.; Moriya, M.; Ishihara, A.; Iwaasa, H.; Matsushita, H.; Nakase, K.; Wallace, M. A.; Dean, D.; Sato, N.; Tokita, S.; Kanatani, A. Identification and characterization of a selective radioligand for melanin-concentrating hormone 1-receptor (MCH1R). *Bioorg. Med. Chem. Lett..* **2009**, *19*, 2835-2839. c) Ito, M.; Ishihara, A.; Gomori, A.; Egashira, S.; Matsushita, H.; Mashiko,

S.; Ito, J.; Ito, M.; Nakase, K.; Haga, Y.; Iwaasa, H.; Suzuki, T.; Ohtake, N.; Moriya, M.; Sato, N.; MacNeil, D. J.; Takenaga, N.; Tokita, S.; Kanatani, A. Melanin-concentrating hormone 1-receptor antagonist suppresses body weight gain correlated with high receptor occupancy levels in diet-induced obesity mice. *Eur. J. Pharmacol.* **2009**, *624*, 77-83.

28. a) Lagu, B.; Wetzel, J.; Marzabadi, M. R.; Deleon, J. E.; Gluchowski, C.; Noble, S.; Nagarathnam, D.; Chiu, G. Preparation and use of arylpyrimidines as selective melanin concentrating hormone-1 (mch-1) receptor antagonists. WO2002006245, January 24, 2002. b) Goss, J. M.; Schaus, S. E. Enantioselective synthesis of SNAP-7941: chiral dihydropyrimidone Inhibitor of MCH1-r. *J. Org. Chem.* **2008**, *73*, 7651-7656.

29. Cavalli, A.; Poluzzi, E.; De Ponti, F.; Recanatini, M. Toward a pharmacophore for drugs inducing the long QT syndrome: insights from a CoMFA study of HERG K+ channel blockers. *J. Med. Chem.* **2002**, *45*, 3844-3853.

30. Washburn, W. N.; Manfredi, M.; Devasthale, P.; Zhao, G.; Ahmad, S.; Hernandez, A.; Robl, J. A.; Wang, W.; Mignone, J.; Wang, Z.; Ngu, K.; Pelleymounter, M. A.; Longhi, D.; Zhao, R.; Wang, B.; Huang, N.; Flynn, N.; Azzara, A. V.; Barrish, J. C.; Rohrbach, K.; Devenny, J. J.; Rooney, S.; Thomas, M.; Glick, S.; Godonis, H. E.; Harvey, S. J.; Cullen, M. J.; Zhang, H.; Caporuscio, C.; Stetsko, P.; Grubb, M.; Maxwell, B. D.; Yang, H.; Apedo, A.; Gemzik, B.; Janovitz, E. B.; Huang, C.; Zhang, L.; Freeden, C.; Murphy, B. J. Identification of a nonbasic melanin hormone receptor 1 antagonist as an antiobesity clinical candidate. *J. Med. Chem.* **2014**, *57*, 7509-7522.

31. Hoegberg, T.; Stroem, P.; Ebner, M.; Raemsby, S. Cyanide as an efficient and mild catalyst in the aminolysis of esters. *J. Org. Chem.* **1987**, *52*, 2033-2036.

32. Ulven, T.; Frimurer, T. M.; Receveur, J.-M.; Little, P. B.; Rist, O.; Norregaard, P. K.; Hoegberg, T. 6-Acylamino-2-aminoquinolines as potent melanin-concentrating hormone 1 receptor antagonists. Identification, structure-activity relationship, and investigation of binding mode. *J. Med. Chem.* **2005**, *48*, 5684-5697.

33. Rivera, G.; Bocanegra-Garcia, V.; Galiano, S.; Cirauqui, N.; Ceras, J.; Perez, S.; Aldana, I.; Monge, A. Melanin-concentrating hormone receptor 1 antagonists: a new perspective for the pharmacologic treatment of obesity. *Curr. Med. Chem.* **2008**, *15*, 1025-1043.

34. Bostrom, J.; Greenwood, J. R.; Gottfries, J. Assessing the performance of OMEGA with respect to retrieving bioactive conformations. *J. Mol. Graphics Modell.* **2003**, *21*, 449-462.

35. Bostrom, J.; Hogner, A.; Llinas, A.; Wellner, E.; Plowright, A. T. Oxadiazoles in medicinal chemistry. *J. Med. Chem.* **2012**, *55*, 1817-1830.

36. Wan, H.; Holmen, A.; Nagard, M.; Lindberg, W. Rapid screening of pKa values of pharmaceuticals by pressure-assisted capillary electrophoresis combined with short-end injection. *J. Chromatogr. A* **2002**, *979*, 369-377.

37. Davis, A. M.; Wood, D. J. Quantitative structure-activity relationship models that stand the test of time. *Mol. Pharm.* **2013**, *10*, 1183-1190.

38. a) Carreira, E. M.; Fessard, T. C. Four-membered ring-containing spirocycles: synthetic strategies and opportunities. *Chem. Rev.* **2014**, *114*, 8257-8322. b) Wuitschik, G.; Rogers-Evans, M.; Buckl, A.; Bernasconi, M.; Marki, M.; Godel, T.; Fischer, H.; Wagner, B.; Parrilla, I.; Schuler, F.; Schneider, J.; Alker, A.; Schweizer, W. B.; Muller, K.; Carreira, E. M. Spirocyclic oxetanes: synthesis and properties. *Angew. Chem. Int. Ed. Engl.* **2008**, *47*, 4512-4515.

39. AZD1979 was tested against more than 250 other receptors, ion channels and enzymes from a wide variety of different target classes. Apart from an IC50 of 400 nM on the H3 receptor, no other confirmed activity below 1 μM could be established.

40. Johansson, L. A. M.; Judkins, R. A.; Li, L.; Lofberg, B. C. I.; Persson, J. Preparation of (azetidinyl)oxadiazolylmethanone derivatives for use as MCH1 receptor modulators. WO2010125390, April 29, 2010.

41. ClinicalTrials.gov Identifier: NCT02072993

42. Dost, J.; Heschel, M.; Stein, J. Preparation of 1,3,4-oxadiazole-2-carboxylic acid derivatives. *J. Prakt. Chem.* **1985**, *327*, 109-116.

43. Borowsky, B.; Durkin, M. M.; Ogozalek, K.; Marzabadi, M. R.; DeLeon, J.; Heurich, R.; Lichtblau, H.; Shaposhnik, Z.; Daniewska, I.; Blackburn, T. P.; Branchek, T. A.; Gerald, C.; Vaysse, P. J.; Forray, C. Antidepressant, anxiolytic and anorectic effects of a melanin-concentrating hormone-1 receptor antagonist. *Nat. Med. (N. Y., NY, U. S.).* **2002**, *8*, 825-830.

44. Lemurell, M.; Ulander, J.; Winiwarter, S.; Dahlen, A.; Davidsson, O.; Emtenaes, H.; Broddefalk, J.; Swanson, M.; Hovdal, D.; Plowright, A. T.; Pettersen, A.; Ryden-Landergren, M.; Barlind, J.; Llinas, A.; Hersloef, M.; Drmota, T.; Sigfridsson, K.; Moses, S.; Whatling, C. Discovery of AZD6642, an inhibitor of 5-lipoxygenase activating protein (FLAP) for the treatment of inflammatory diseases. *J. Med. Chem.* **2015**, *58*, 897-911.

Table of Contents graphic

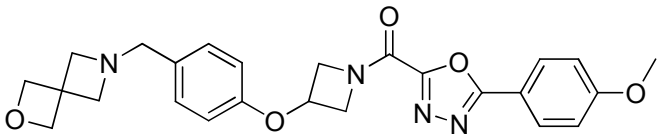

103

LogD=2.0, pKa=8.2

Ki MCHr1 (GTPγS) = 5.2 ± 0.3 nM; Ki MCHr1 (Binding) = 12.2 ± 1.4 nM

IC_{50} MCHr2 IC_{50}>40 μM; hERG= 22 μM